

## Supporting Information

### One-year post-exposure assessment of $^{14}\text{C}$ -few-layer graphene biodistribution in mice: single versus repeated intratracheal administration.

Antoine Sallustrau,<sup>a,\*</sup> Mathilde Keck,<sup>b,\*</sup> Peggy Barbe,<sup>b</sup> Dominique Georjin,<sup>a</sup> Nathalie Fresneau,<sup>c,a</sup> Stephane Campidelli,<sup>c</sup> Baptiste Pibaleau,<sup>d</sup> Mathieu Pinault,<sup>d</sup> Martine Mayne-L'Hermite,<sup>d</sup> Christine Granotier-Beckers,<sup>e</sup> Michel Schlegel,<sup>f</sup> Viviana Jehová González,<sup>g</sup> Ester Vázquez,<sup>g</sup> Denis Servent,<sup>b</sup> Frédéric Taran.<sup>a</sup>

- a. Université Paris Saclay, CEA, INRAE, Département Médicaments et Technologies pour la Santé (DMTS), SCBM, 91191 Gif-sur-Yvette, France.
- b. Université Paris Saclay, CEA, INRAE, Département Médicaments et Technologies pour la Santé (DMTS), SIMos, 91191 Gif-sur-Yvette, France.
- c. Université Paris-Saclay, CEA, CNRS, NIMBE, LICSEN, 91191 Gif-sur-Yvette, France.
- d. Université Paris-Saclay, CEA, CNRS, NIMBE, LEDNA, 91191 Gif-sur-Yvette, France
- e. Université Paris Cité, Inserm, CEA, Stabilité Génétique Cellules Souches et Radiations/iRCM, 92265 Fontenay-aux-Roses, France; Université Paris-Saclay, Inserm, CEA, Stabilité Génétique Cellules Souches et Radiations/iRCM, 92265 Fontenay-aux-Roses, France
- f. Université Paris Saclay, CEA, Service de Recherche en Matériaux et Procédés Avancés, 91191 Gif-sur-Yvette, France
- g. Instituto Regional de Investigación Científica Aplicada (IRICA), Universidad de Castilla-La Mancha, 13071 Ciudad Real, Spain.

## **1. Method**

## **2. $^{12}\text{C}$ and $^{14}\text{C}$ -Graphite**

### **2.1. Synthesis**

### **2.2. Characterization**

- A. Electron Microscopy analysis of  $^{12}\text{C}$ -Graphite with and without Nickel foam.
- B. Raman Analysis of  $^{12}\text{C}$ -Graphite and  $^{14}\text{C}$ -Graphite
- C. XPS analysis of  $^{12}\text{C}$ -Graphite.
- D. Thermogravimetric analysis of  $^{12}\text{C}$ -Graphite

## **3. $^{12}\text{C}$ and $^{14}\text{C}$ -Few-Layer Graphene**

### **3.1. Synthesis**

### **3.2. Characterization**

- A. Raman Analysis of  $^{12}\text{C}$ -Graphite and  $^{14}\text{C}$ -Graphite
- B. Thermogravimetric analysis of  $^{12}\text{C}$ -Few-Layer Graphene
- C. UV analysis of the  $^{12}\text{C}$ -FLG suspension.

## **4. Biodistribution**

### **4.1. Whole-body localization**

### **4.2. Organs distribution**

### **4.3. Elimination**

### **4.4. Cellular localization**

### **4.5. Toxicity**

# 1. Method

## 1.1. Autoradiography

**HeLa culture and <sup>14</sup>C-FLG exposition.** HeLa (epithelial cells from human cervical adenocarcinoma) were cultured at  $2 \cdot 10^5$  cells/T75 cm<sup>2</sup> flask in DMEM medium supplemented with 10% fetal bovine serum (FBS, Gibco Life Technologies), 2 mM glutamine (Gibco Life Technologies) and antibiotics (100 U.mL<sup>-1</sup> penicillin and 100 µg.mL<sup>-1</sup> streptomycin, Gibco Life Technologies). At each passage, cells were harvested by trypsinization and re-seeded with 10 mL of fresh medium. For experiments with <sup>14</sup>C-FLG, HeLa cells were plated in 8-well Lab-Tek chamber slide (Nunc) and cultured during 24 hours ( $2 \cdot 10^4$  cells/well with 500 µL of culture medium) at 37 °C with 5% CO<sub>2</sub>. The nanomaterials (0 to 1.6 kBq of <sup>14</sup>C-FLG) were then diluted in the culture medium, and subsequently, the cells were exposed for 24 hours. The cells were then washed with PBS twice, fixed with 4% PFA (Paraformaldehyde, Chem Cruz) for 1 hour at room temperature and washed with PBS to remove traces of PFA. The dehydration step was performed by successive ethanol solutions (70%, 90% and 100 %) for 1 min each and the cells were dried for 1 hour, before analysis by µ-autoradiography.

**Radiosensitive emulsion exposition.** In a dark room under inactinic light (Ilford Orange DL10 filter), the radiosensitive emulsion jar (Emulsion NTB autoradiography, Carestream Ref 8895666, Valdea Bioscience) was placed in a water bath heated up to 42°C for 30 to 45 min. The liquefied radiosensitive emulsion was gently homogenized. The emulsion was then diluted to 2/3 using Milli-Q water: in a 50 mL Falcone, 6.6 mL of preheated H<sub>2</sub>O (42°C) and 10 mL of the warm emulsion were combined to provide enough emulsion to treat 10 slides. Using a specific piece of glass (Fig. S24), the slides were gently dipped in the emulsion and removed carefully to avoid bubbles formation. A single dip in the emulsion was enough to cover the entire slide. The back of the slides were wiped with a paper towel and the slide were then dried for 2 hours in a horizontal position under an opaque cover. The slides were then stored at 4°C for the desired time in a black plastic box containing silica-gel in the lid and wrapped with aluminum foil to avoid any exposition to light.

**Radiosensitive emulsion development.** In the darkroom under inactinic light, the slides were dipped successively into 200 mL of developer (Kodak D19 Developer Ref 1464593) for 4.5 min, 30 sec in 200 mL of a STOP solution (4 mL acetic solution, qsp 200 mL with H<sub>2</sub>O) and 10 min in 200 mL of fixative solution (Kodak Fixative 1971746). Once fixed, the slides could then be exposed to light. The slides were finally rinsed for 10 to 20 min with tap water.

**Tissue staining.** Slides were immersed in pure Mayer's hemalum (Merck) dye for 5 min at room temperature and washed with tap water until the liquid that flows out was colorless (15 min). The dehydration step was carried out using successive ethanol solutions (70%, 90%, 95%, 100%) into which the slide was dipped for 1 minute. The slides were then air dried.

**Slide mounting and analysis.** Slides were mounted with a drop of Eukitt was placed on the slide and the slides were dried between 1 and 2h under a fumehood.

**Data processing.** Quantitative data are shown as means, with error bars indicating the standard error of the mean (SEM). The number of animals or samples used is indicated in each figure legend. Comparisons between more than two groups were performed using the Kruskal-Wallis non-parametric test followed by Dunn's multiple comparisons test. To compare repeated measurements over time, we used the non-parametric mixed-effects model followed by Dunnett's multiple comparisons test. Differences were considered significant if *P* value was < 0.05. Statistical analyses and figures were performed using GraphPad Prism 9 software (GraphPad software Inc, San Diego, CA, USA).

## 2. Graphite

### 2.1. Synthesis



Figure S1. Chemical Vapor Deposition set-up

### 2.2. Characterization

A. Electron Microscopy analysis of  $^{12}\text{C}$ -Graphite with and without Nickel foam. Graphite was analysed by electron microscopy (SEM, STEM and TEM).

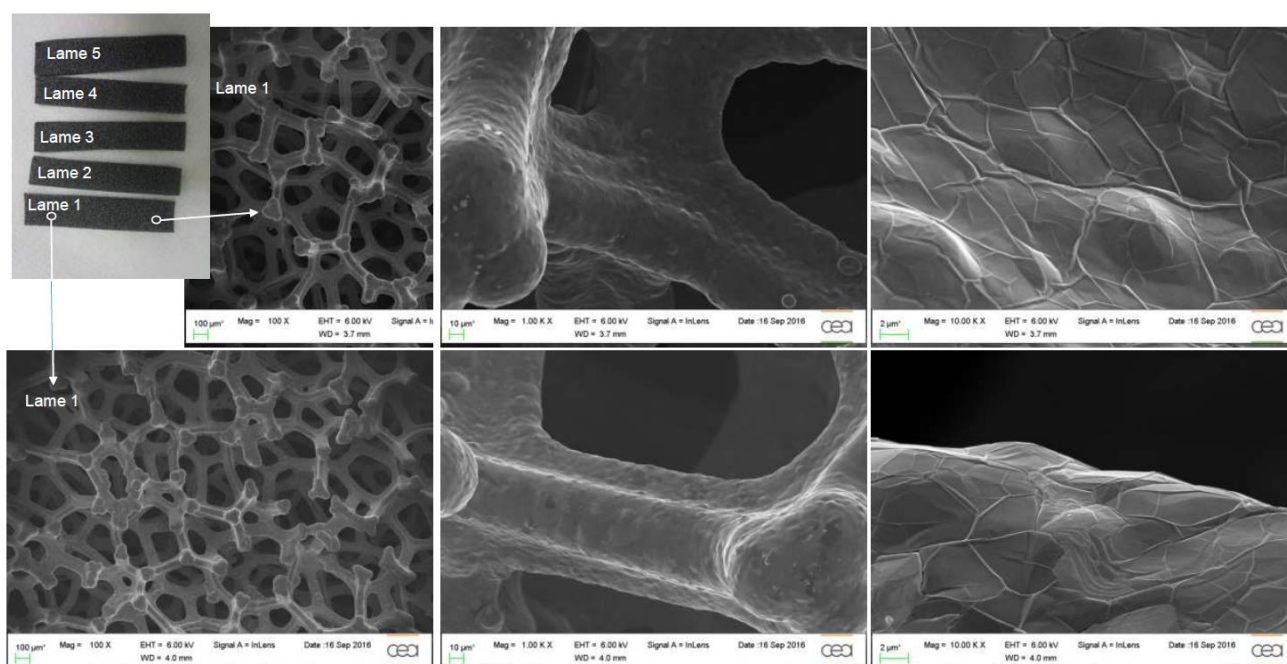
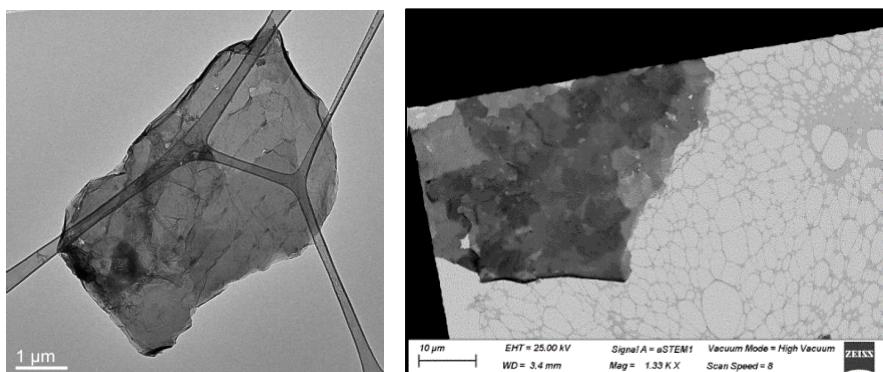


Figure S2. Scanning electron microscopy analysis of  $^{12}\text{C}$ -Graphite on Nickel foam



**Figure S3.** Transmission electron microscopy (left) and Scanning transmission electron microscopy (right) analysis of  $^{12}\text{C}$ -Graphite after dissolution of the Nickel foam

## B. Raman Analysis of $^{12}\text{C}$ -Graphite and $^{14}\text{C}$ -Graphite

**$^{12}\text{C}$ -Graphite.** Raman spectra were recorded on a LabRam HR800 spectrometer equipped with an Olympus microscope and a 50× long-range objective.

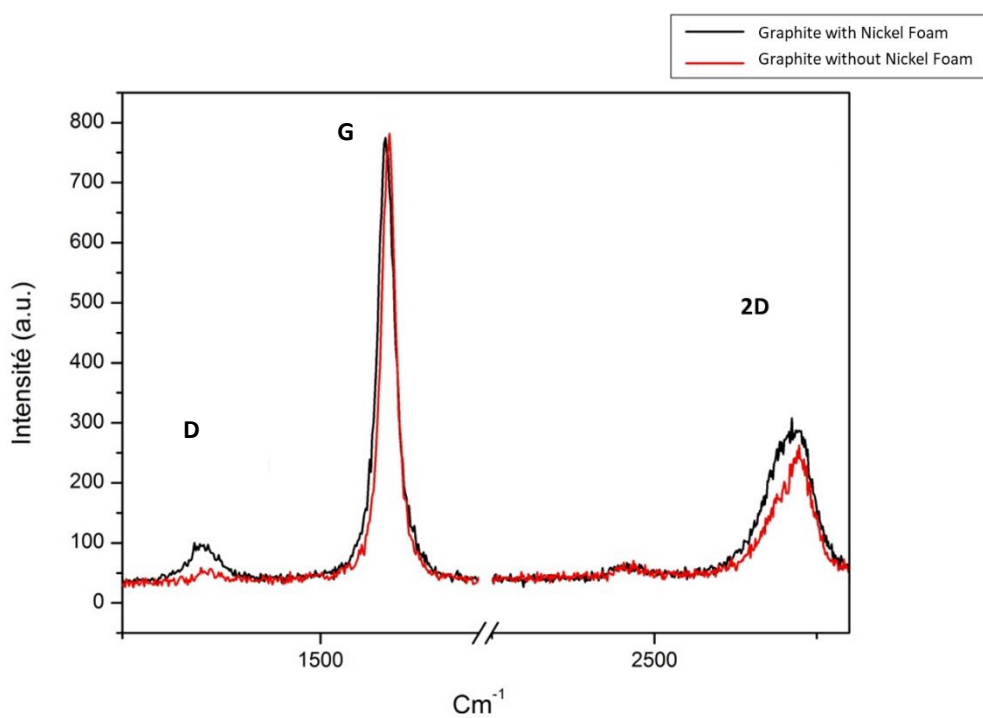


**Figure S4.** Overlay of Raman Analysis of  $^{12}\text{C}$ -Graphite with (black) and without Nickel Foam (red)

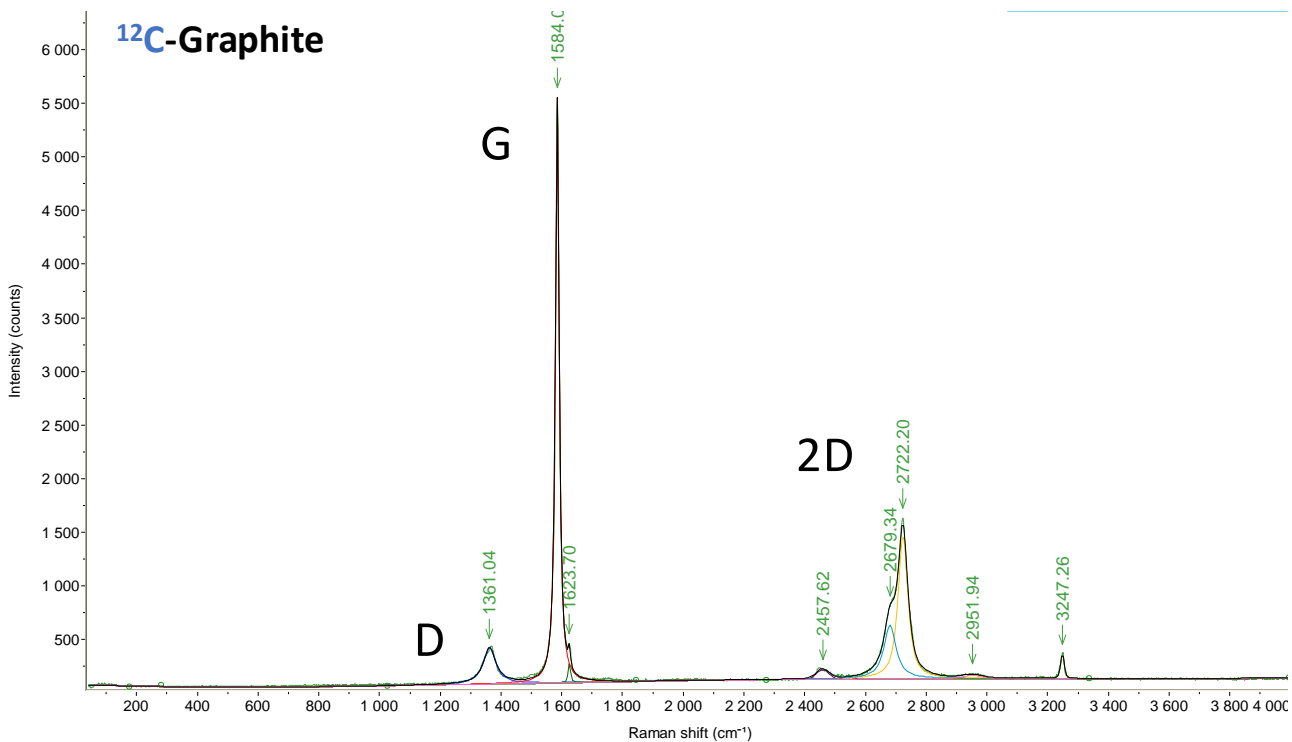


Figure S5. Raman Analysis of <sup>12</sup>C-Graphite

**<sup>14</sup>C-Graphite.** Raman spectra were recorded on a LabRam HR800 spectrometer equipped with an Olympus microscope and a 50× long-range objective.

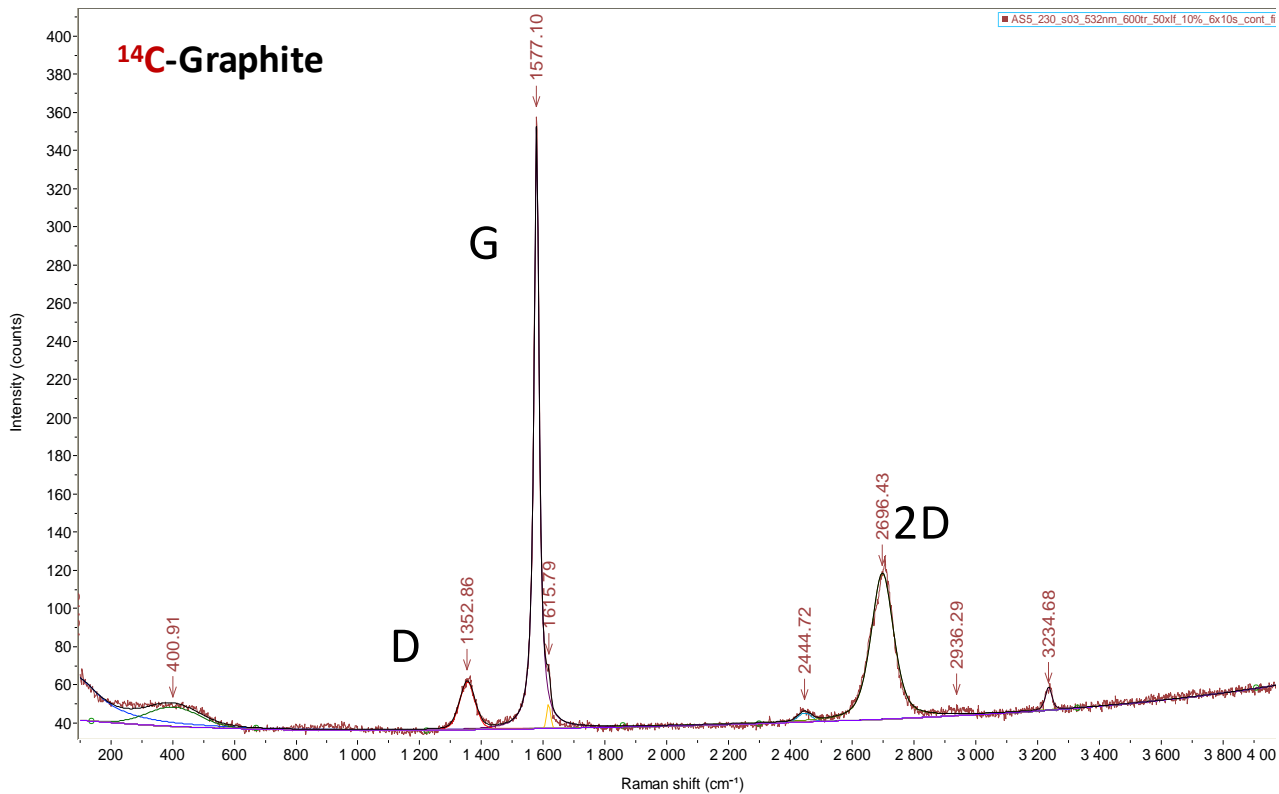
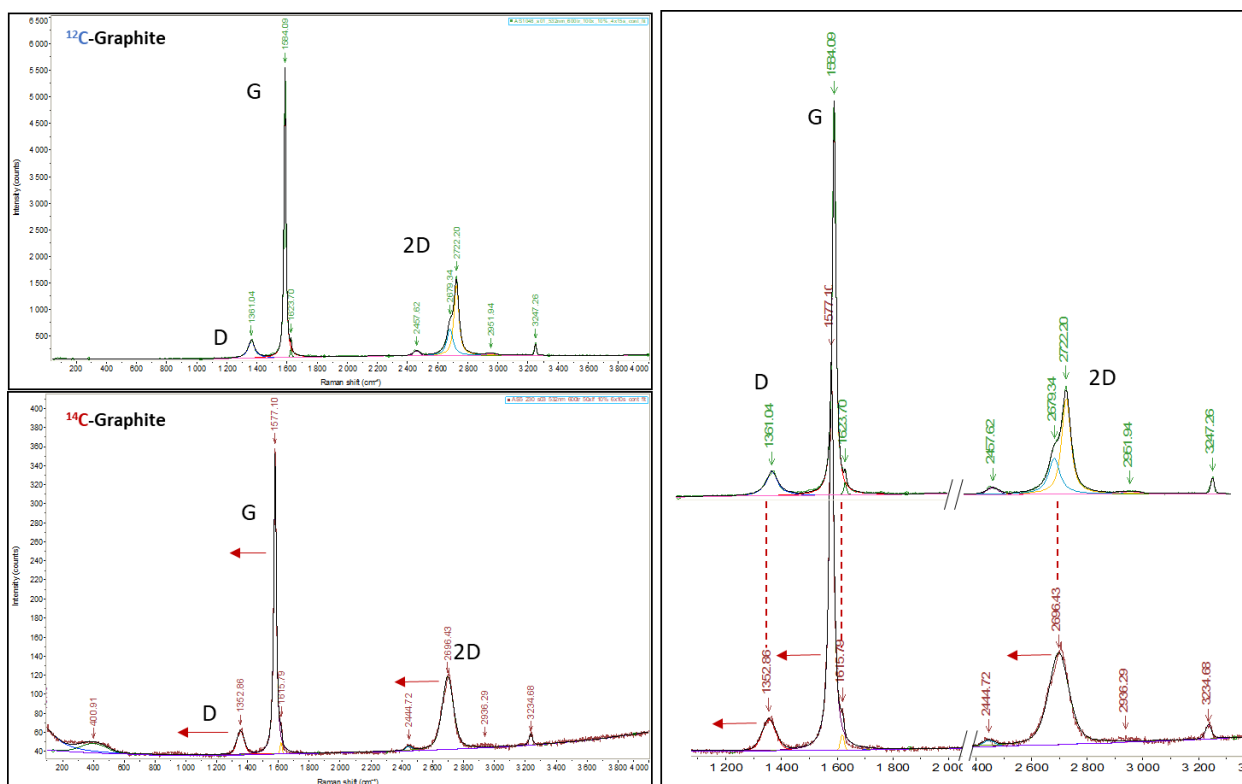


Figure S6. Raman Analysis of <sup>14</sup>C-Graphite



**Figure S7.** Left panel. Overlay of Raman spectra of  $^{12}\text{C}$ -Graphite with (up) and  $^{14}\text{C}$ -Graphite (down). Right panel. Overlay of both spectra.

**Determination of the isotope enrichment of  $^{14}\text{C}$ -Graphite using the following equation:**

$$\frac{(\omega_0 - \omega)}{\omega_0} = 1 - \sqrt{\frac{12 + c_0}{12 + c}}$$

**Equation S1.** Equation used for the determination of isotope enrichment where  $\omega_0$  is the frequency of the  $^{12}\text{C}$  sample,  $\omega$  corresponds to the frequency of the  $^{14}\text{C}$  sample,  $c$  corresponds to the concentration of  $^{14}\text{C}$  in the enriched sample, and  $c_0 = 1/10^{12}$  is the natural abundance of  $^{14}\text{C}$ .

**C. XPS analysis of  $^{12}\text{C}$ -Graphite.** The chemical composition of the non-radiolabelled Graphite was evaluated by XPS (X-ray induced photoelectron spectroscopy) analysis using a Kratos Analytical Axis Ultra DLD spectrometer with monochromatic Al KR X-ray radiation ( $h\nu = 1486.6 \text{ eV}$ ). Quantitative analysis of Graphite indicated that the C content was ca. 97.9 %, the O content was ca. 2.1 %. No nitrogen contribution was observed.

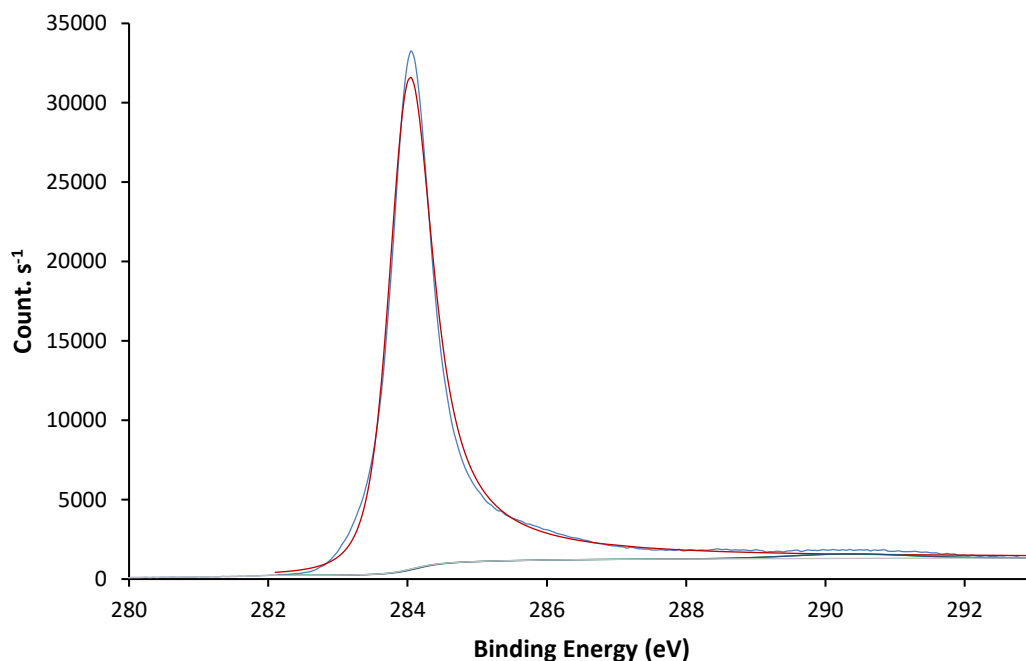


**Figure S8.** XPS analysis of Carbon composition in  $^{12}\text{C}$ -Graphite indicating a content of 97.9 %

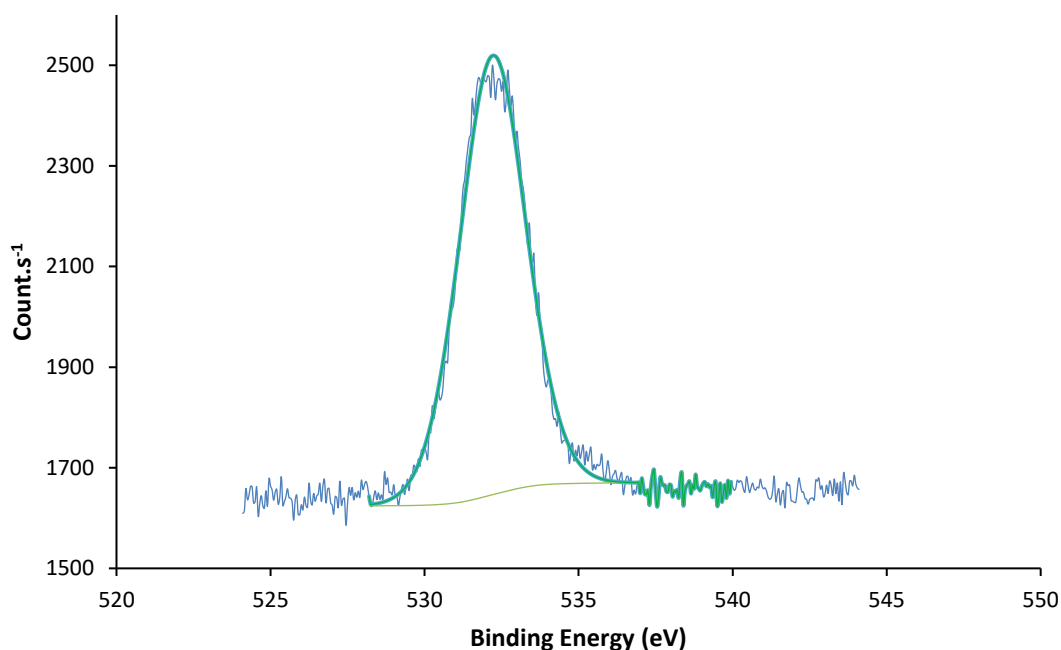


**Figure S9.** XPS analysis of Oxygen composition in  $^{12}\text{C}$ -Graphite indicating a content of 2.1 %

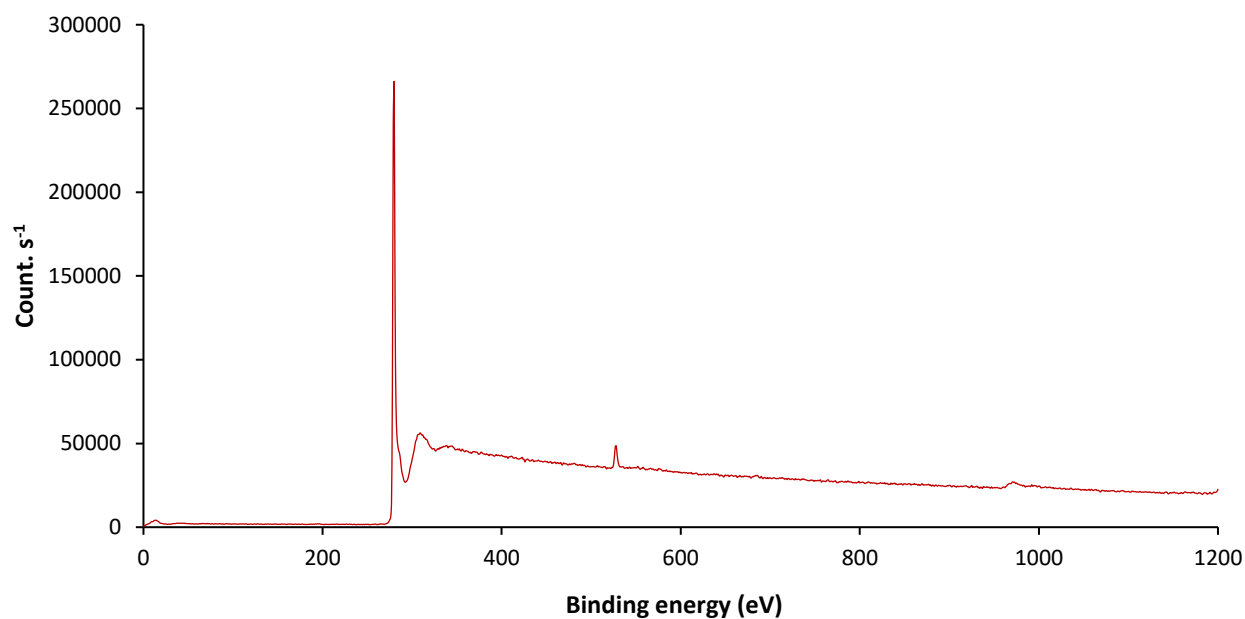


Figure S10. XPS survey spectra of <sup>12</sup>C-Graphite

#### D. Thermogravimetric analysis of <sup>12</sup>C-Graphite.

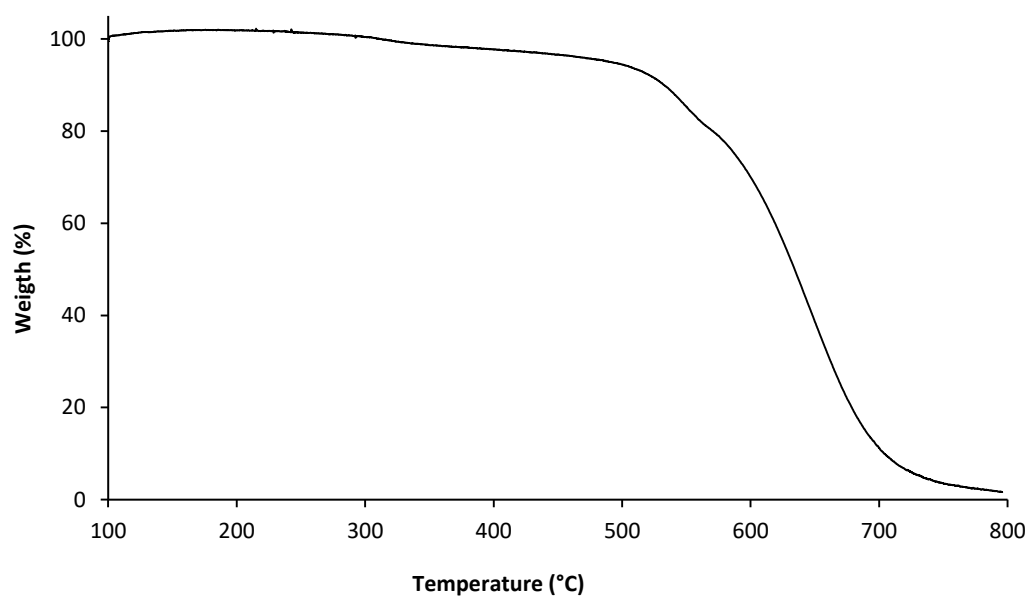
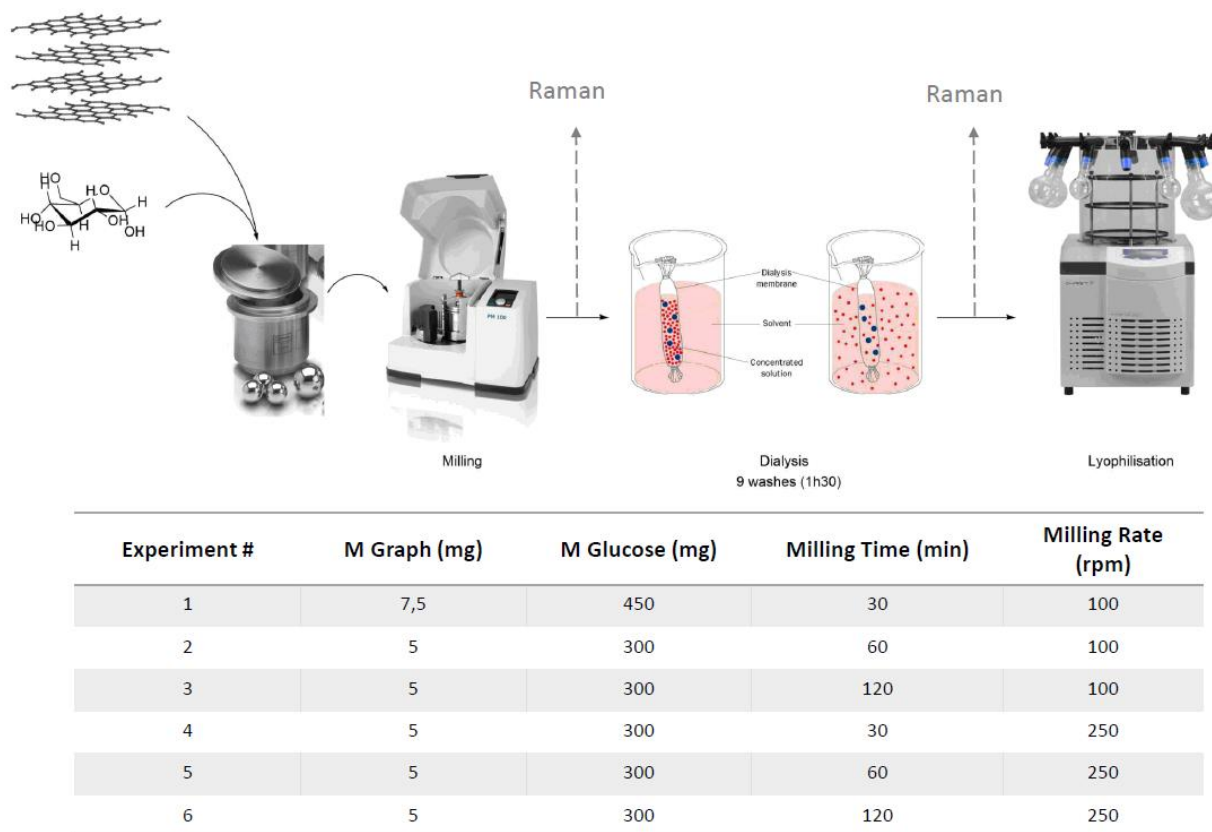


Figure S11. Thermogravimetric analysis of <sup>12</sup>C-Graphite under air

# 1. Few-Layer Graphene

## 1.1. Synthesis



**Figure S12.** Schematic representation of the different step for the preparation of FLG and the optimisations test

### Optimization test for the exfoliation of $^{12}\text{C}$ -graphite into $^{12}\text{C}$ -FLG

In the following tables S1 and S2 are presented characteristic parameters obtained from the Raman characterization of the different trials performed on 5 mg scale graphite samples. Time and speed have been screened. Three times and 2 speeds have been considered: 30 minutes, 1 hour and 2 hours for 100 rpm and 250 rpm. With the goal to reach few layers graphene material, we based our screening on the number of layers which is correlated to the value of Full Width at Half Maximum (FWHM) in the 2D band.<sup>1</sup> After 2 hour of milling, we observed a significant reduction in the number of layers, in line with previous research.<sup>2</sup> Additionally, by increasing the milling speed we achieve a 6 layers graphene representing the most favourable outcome among the various synthesis conditions we explored. As for defects, there was an increase corresponding to the relationship between the D and G bands.

**Table S1.** Results obtained for the Raman spectra of the samples after exfoliation at 100 rpm.

Global sample																
	ID/IG	I2D/IG	FWHD	G'=2D	G	D	I2D	IG	ID	ID'	ID/ID'	I-2718,00-wp	I-2685,83-ws	M	NG	
Graphite	0,18	0,35	69,12	2707,21	1582,42	1355,46	0,34	0,97	0,17	0,05	3,21	0,35	0,27	1,28	1,00	19,50
30min	0,21	0,43	66,46	2708,32	1581,76	1351,28	0,42	0,98	0,21	0,06	3,53	0,43	0,33	1,31	1,02	21,01
30min after cleaning	0,17	0,35	65,23	2708,51	1581,58	1352,62	0,34	0,98	0,17	0,05	3,19	0,34	0,28	1,20	0,93	15,04
1H	0,29	0,42	66,19	2705,47	1581,03	1348,50	0,41	0,98	0,28	0,07	3,97	0,40	0,33	1,21	0,94	15,66
1H after cleaning	0,39	0,46	66,90	2703,62	1581,25	1348,57	0,45	0,97	0,38	0,10	3,82	0,43	0,39	1,12	0,87	11,91
2H	0,54	0,43	66,21	2701,12	1581,47	1348,21	0,42	0,98	0,53	0,14	3,90	0,39	0,38	1,03	0,80	9,15
2H after cleaning	0,49	0,41	66,62	2699,49	1580,46	1347,74	0,41	0,98	0,48	0,12	3,97	0,35	0,35	1,01	0,79	8,70

Graphene part of the sample																
	ID/IG	I2D/IG	FWHD	G'=2D	G	D	I2D	IG	ID	ID'	ID/ID'	I-2718,00-wp	I-2685,83-ws	M	NG	
Graphite	0,18	0,35	69,12	2707,21	1582,42	1355,46	0,34	0,97	0,17	0,05	3,21	0,35	0,27	1,28	1,00	19,50
30min	0,33	0,45	69,11	2704,79	1582,16	1349,74	0,44	0,98	0,32	0,09	3,53	0,42	0,38	1,13	0,88	12,17
30min after cleaning	0,30	0,39	66,69	2705,39	1581,66	1349,71	0,39	0,99	0,30	0,08	3,62	0,37	0,31	1,20	0,94	15,27
1H	0,46	0,45	67,19	2701,22	1581,22	1347,52	0,44	0,98	0,46	0,11	4,20	0,40	0,38	1,04	0,81	9,54
1H after cleaning	0,45	0,48	65,99	2702,58	1581,42	1348,29	0,46	0,97	0,43	0,11	3,83	0,44	0,40	1,09	0,85	11,07
2H	0,65	0,45	65,80	2698,99	1581,53	1347,90	0,44	0,98	0,63	0,16	3,88	0,38	0,40	0,95	0,74	7,44
2H after cleaning	0,55	0,43	66,21	2698,61	1580,78	1347,70	0,42	0,98	0,54	0,14	3,99	0,35	0,37	0,96	0,75	7,65

**Table S2.** Results obtained for the Raman spectra of the samples after exfoliation at 250 rpm

Global sample																
	ID/IG	I2D/IG	FWHD	G'=2D	G	D	I2D	IG	ID	ID'	ID/ID'	I-2718,00-wp	I-2685,83-ws	M	NG	
Graphite	0,181	0,349	69,122	2707,207	1582,422	1355,465	0,337	0,967	0,175	0,054	3,214	0,345	0,269	1,283	1,000	19,50
30min after cleaning	0,452	0,472	65,230	2701,615	1580,920	1350,819	0,463	0,981	0,444	0,076	5,805	0,409	0,394	1,040	0,810	9,45
250 rpm 1H after cleaning	0,448	0,456	66,237	2700,703	1581,268	1349,270	0,454	0,995	0,446	0,129	3,454	0,395	0,388	1,018	0,793	8,89
2H after cleaning	0,834	0,472	67,614	2695,159	1580,793	1347,529	0,464	0,984	0,821	0,189	4,341	0,360	0,423	0,851	0,663	5,69

Graphene part of the sample																
	ID/IG	I2D/IG	FWHD	G'=2D	G	D	I2D	IG	ID	ID'	ID/ID'	I-2718,00-wp	I-2685,83-ws	M	NG	
Graphite	0,181	0,349	69,122	2707,207	1582,422	1355,465	0,337	0,967	0,175	0,054	3,214	0,345	0,269	1,283	1,000	19,50
30min after cleaning	0,453	0,471	65,225	2701,614	1580,916	1350,831	0,463	0,982	0,445	0,076	5,857	0,410	0,392	1,045	0,814	9,61
250 rpm 1H after cleaning	0,452	0,457	66,232	2700,650	1581,286	1349,261	0,454	0,995	0,449	0,130	3,455	0,392	0,383	1,022	0,797	9,01
2H after cleaning	0,837	0,472	67,560	2695,178	1580,814	1347,550	0,464	0,985	0,824	0,190	4,341	0,361	0,424	0,851	0,663	5,69

## 1.2. Characterization

### A. Raman Analysis of $^{12}\text{C}$ -FLG and $^{14}\text{C}$ -FLG.

$^{12}\text{C}$ -FLG. Raman spectra were recorded on a LabRam HR800 spectrometer equipped with an Olympus microscope and a 50× long-range objective.

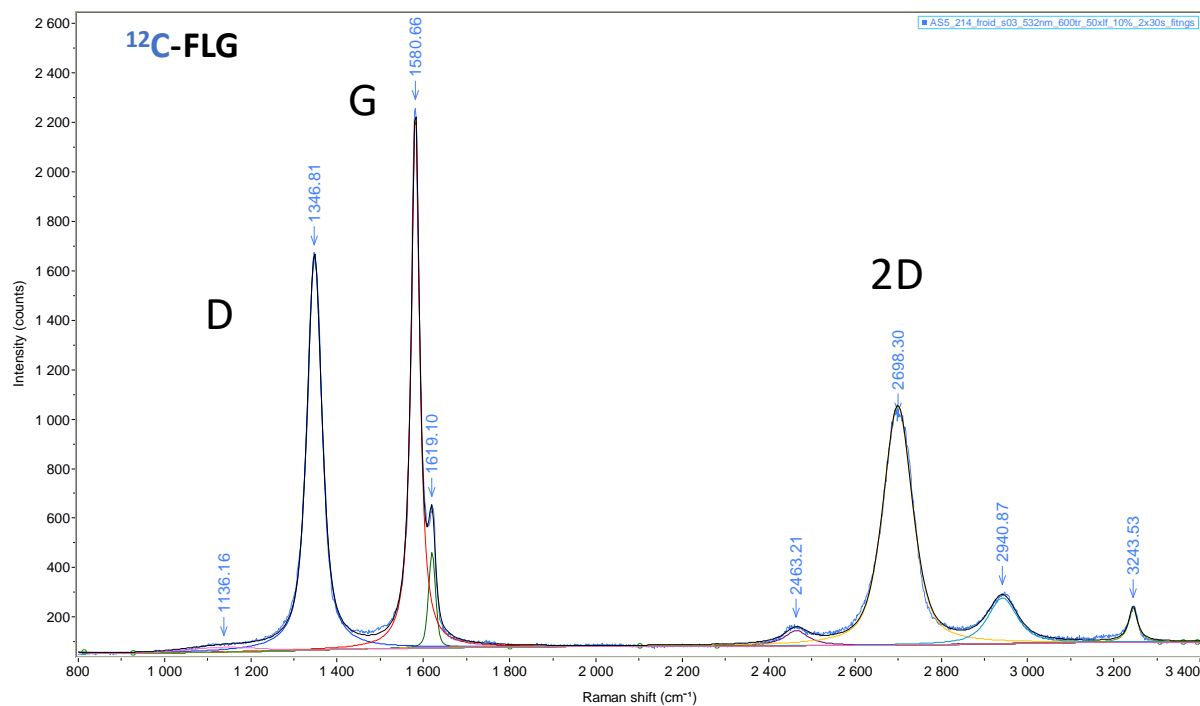


Figure S13. Raman Analysis of  $^{12}\text{C}$ -Few Layer Graphene

$^{14}\text{C}$ -FLG. Raman spectra were recorded on a LabRam HR800 spectrometer equipped with an Olympus microscope and a 50× long-range objective.

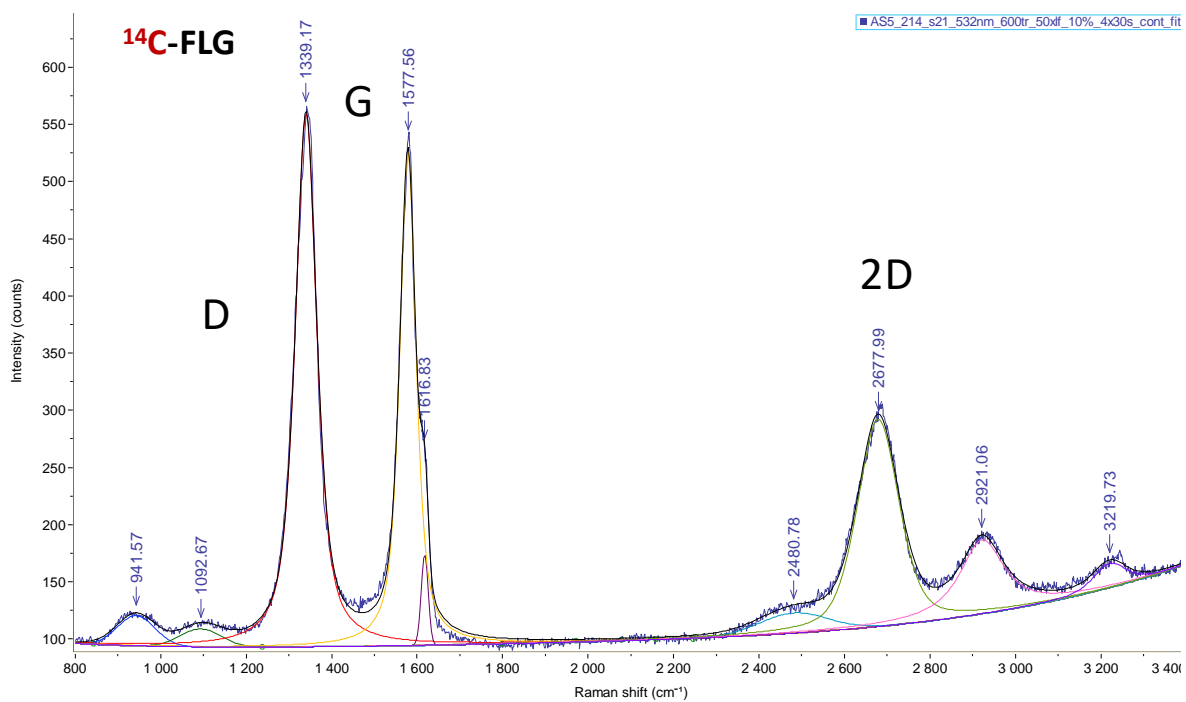


Figure S14. Raman Analysis of  $^{14}\text{C}$ -Few Layer Graphene

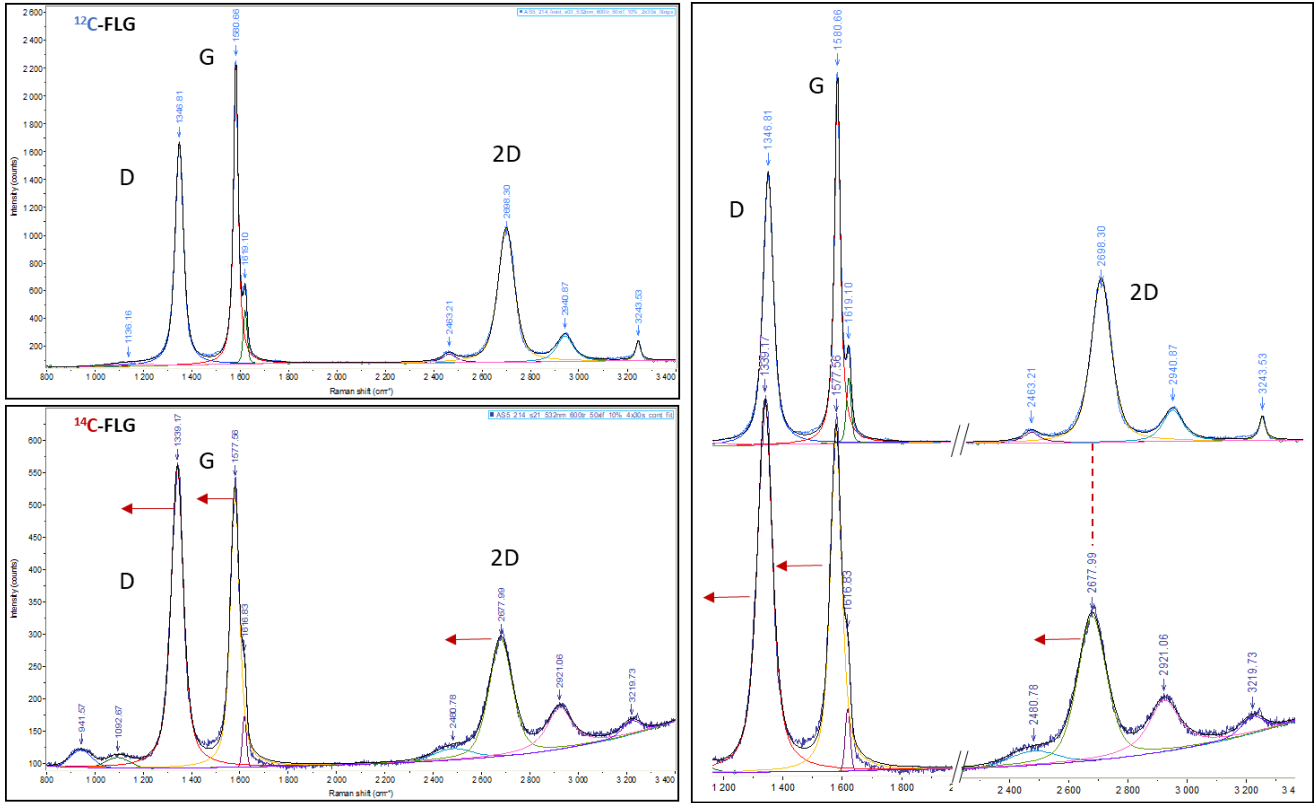


Figure S15. Left panel. Overlay of Raman spectra of  $^{12}\text{C}$ - Few Layer Graphene with (up) and  $^{14}\text{C}$ - Few Layer Graphene (down). Right panel. Overlay of both  $^{12}\text{C}$ - and  $^{14}\text{C}$ -FLG

### Glass Window contribution

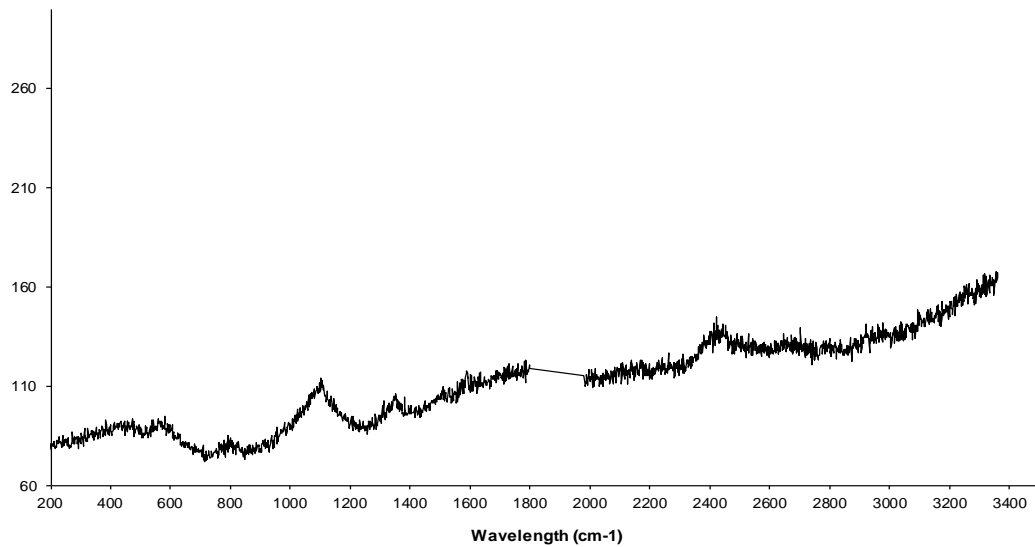


Figure S16. Raman Analysis of the glass window

### Coverslip contribution

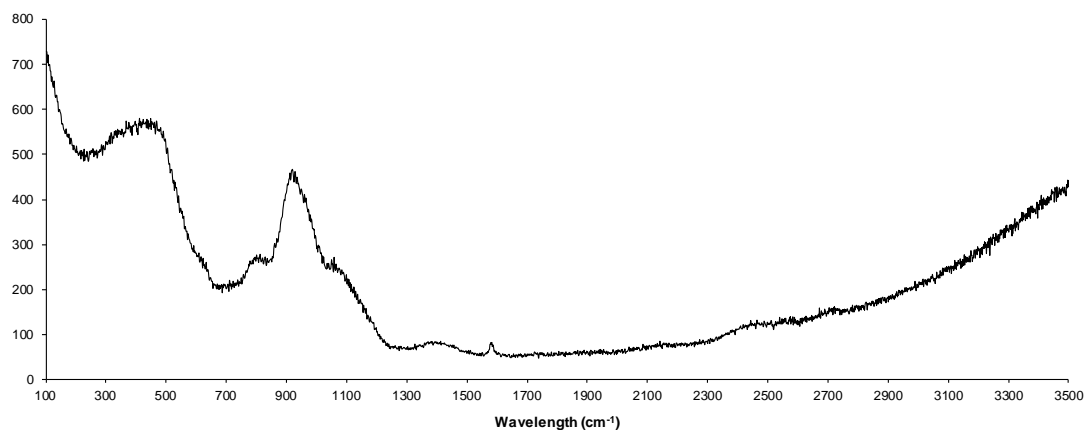


Figure S17. Raman Analysis of the Coverslip

### Container for Raman analysis

A specific container was designed to confine <sup>14</sup>C-Graphite while running the Raman experiment. It was also used to analyse <sup>14</sup>C-FLG.



Figure S18. Container designed to confine <sup>14</sup>C-Graphite while running the Raman experiment

### B. Thermogravimetric Analysis of <sup>12</sup>C-FLG

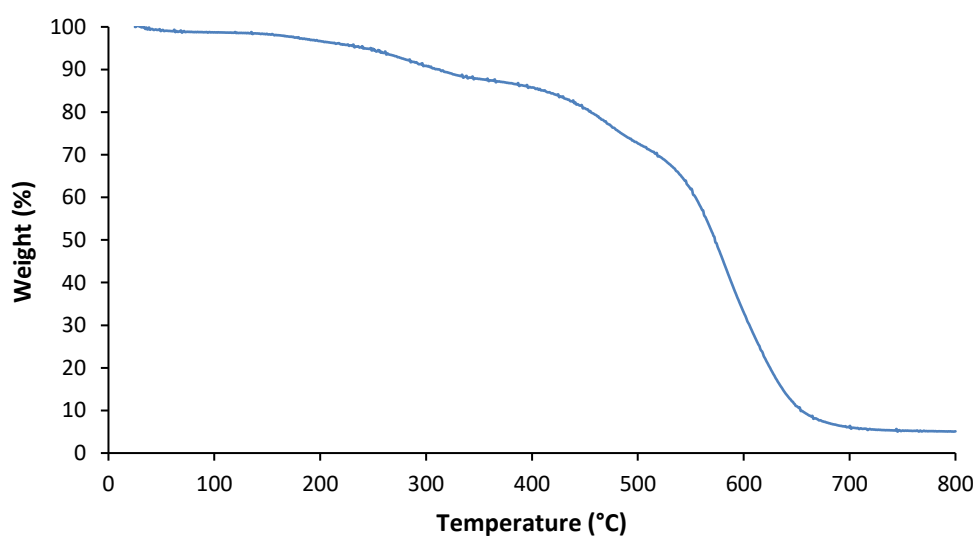


Figure S19. TGA analysis of <sup>12</sup>C-FLG under air

C. UV analysis of the  $^{12}\text{C}$ -FLG suspension.

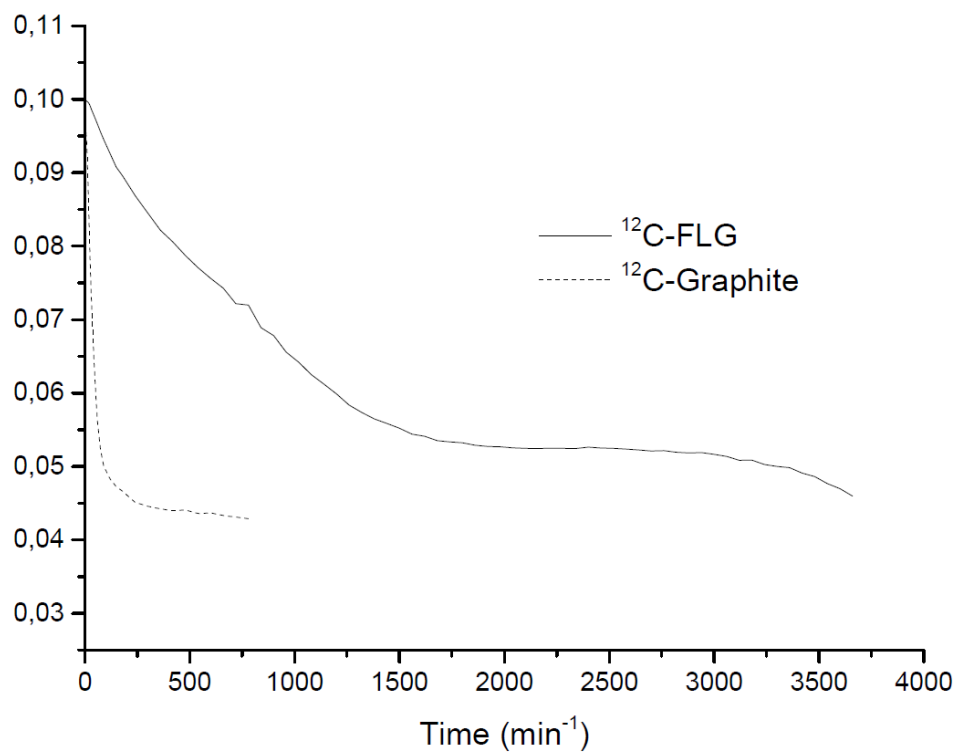
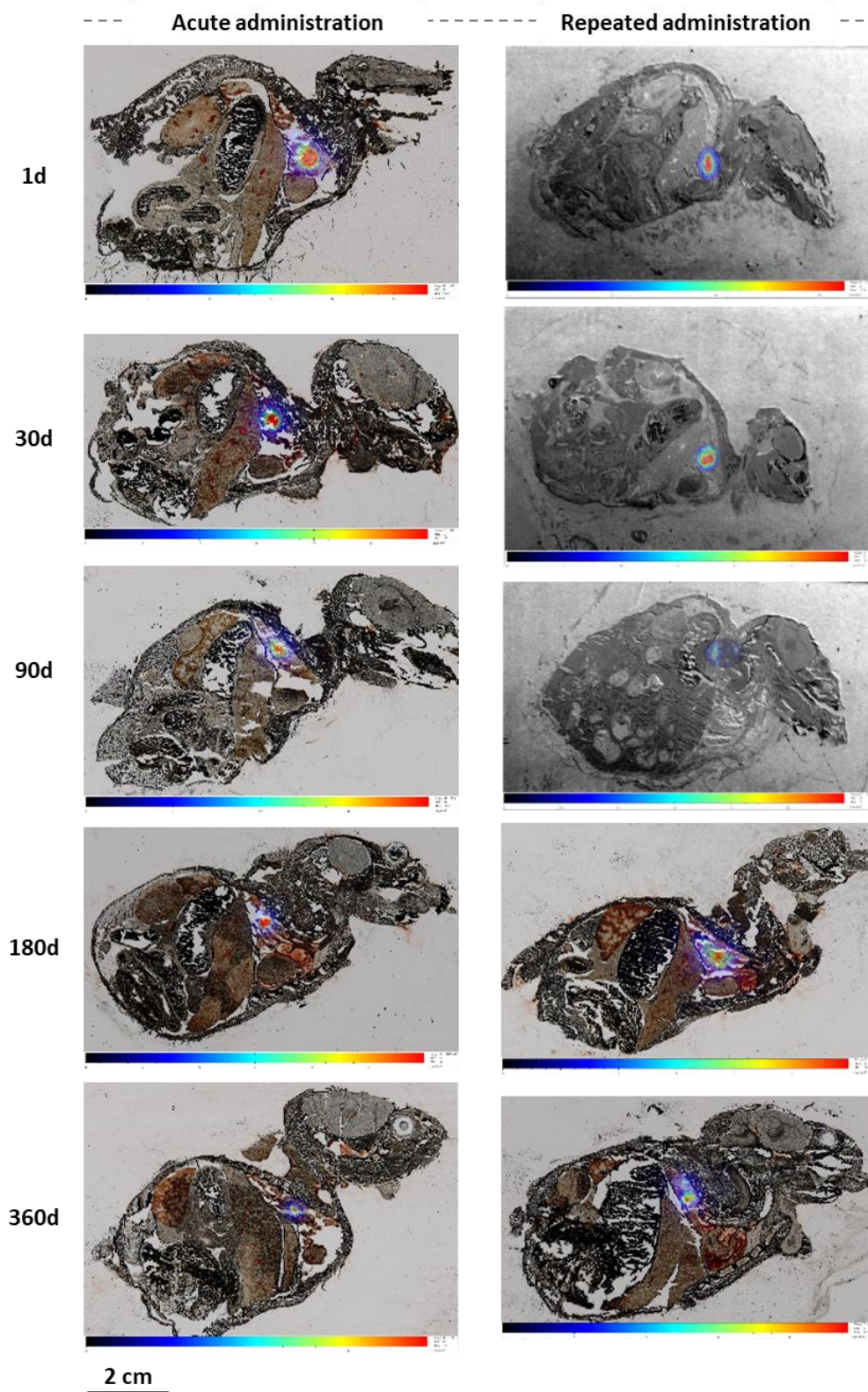


Figure S20. Colloidal stability of  $^{12}\text{C}$ -FLG over time compared to  $^{12}\text{C}$ -Graphite

## 2. Biodistribution

### 2.1. Whole-body localization



**Figure S21.** Whole-body slices (30 μm thick) of female Balb/cJ mice observed by β-imagery after <sup>14</sup>C-FLG acute (left panel) or repeated (right panel) tracheal administration over 360 days. One representative slice over 6 slices per mouse of n=3 mice per time and per group.

## 2.2. Organs distribution

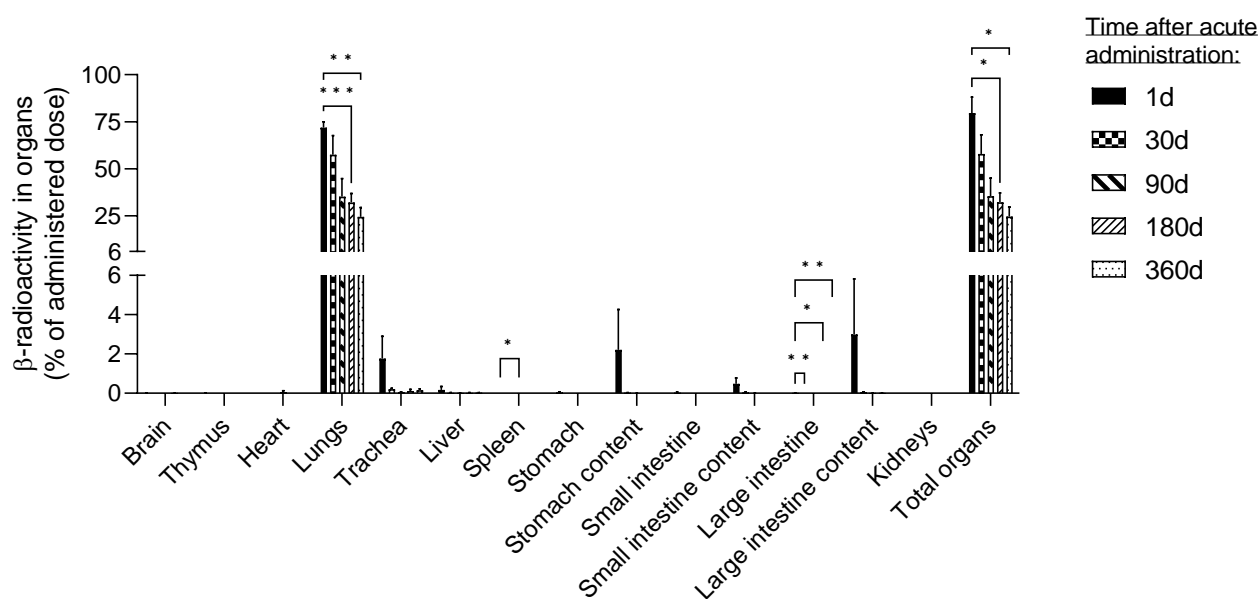


**Figure S22.** Mean  $\pm$  SEM of percentage of organ  $\beta$ -radioactivity administered dose over time following  $^{14}\text{C}$ -FLG acute high-dose tracheal administration.  $n = 5$  female Balb/cj mice per time and per group. Mixed-effects model followed by Dunnett's multiple comparisons test; \*  $p < 0.05$ , \*\*  $p < 0.01$ , \*\*\*  $p < 0.001$  compared to 1d for each organ.

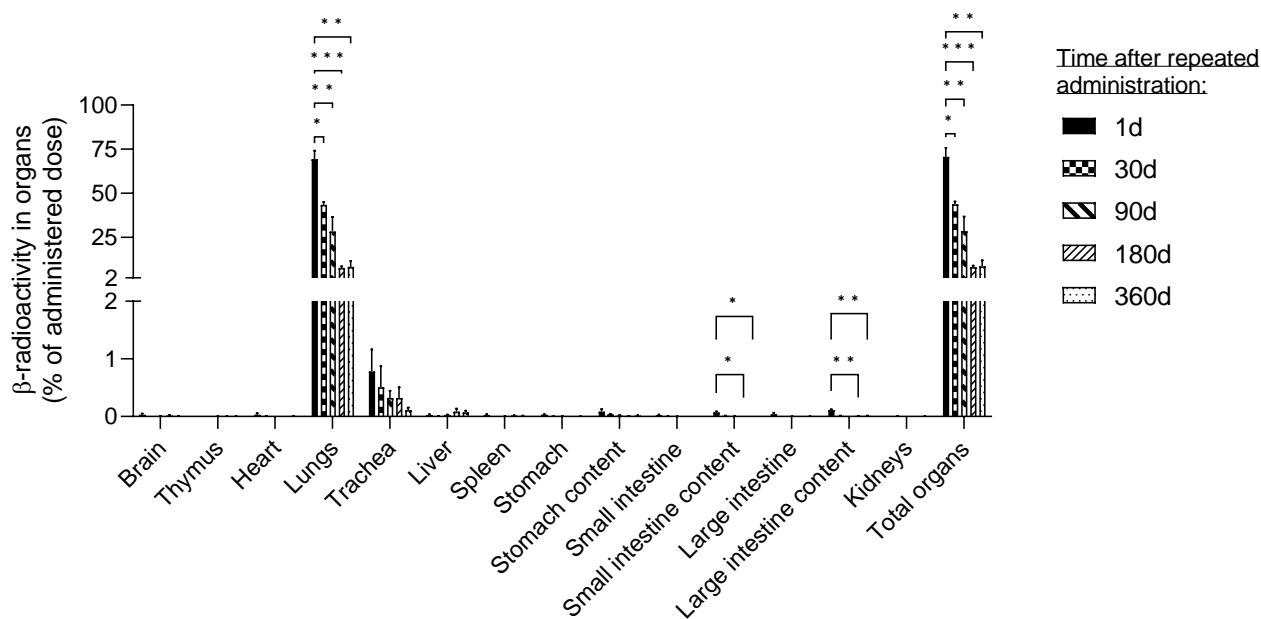


**Figure S23.** Mean  $\pm$  SEM of percentage of organ  $\beta$ -radioactivity administered dose over time following  $^{14}\text{C}$ -FLG repeated low-doses tracheal administration.  $n = 5$  female Balb/cj mice per time and per group. Mixed-effects model followed by Dunnett's multiple comparisons test; \*  $p < 0.05$ , \*\*  $p < 0.01$ , \*\*\*  $p < 0.001$  compared to 1d for each organ.

## 2.3. Elimination

**Table S3.** Mean  $\pm$  SEM of percentage of  $\beta$ -radioactivity administered dose contained in urine or faeces over 30d following  $^{14}\text{C}$ -FLG acute high-dose versus repeated low-doses tracheal administration.  $n = 8$  female Balb/cJ mice per time and per group.

	Acute high-dose of $^{14}\text{C}$ -FLG		Repeated low-doses of $^{14}\text{C}$ -FLG	
	0 to 1 day after admin.	1 day to 30 days after admin.	-28 to 1 day after admin.	1d to 30d after admin.
% of $\beta$ -radioactivity administered dose in urine	0.10 $\pm$ 0.04	0.01 $\pm$ 0.01	0.03 $\pm$ 0.003	0.04 $\pm$ 0.003
% of $\beta$ -radioactivity administered dose in faeces	18.23 $\pm$ 8.74	38.14 $\pm$ 2.85	22.78 $\pm$ 0.41	41.15 $\pm$ 1.50

## 2.4. Cellular localization

### a. Material

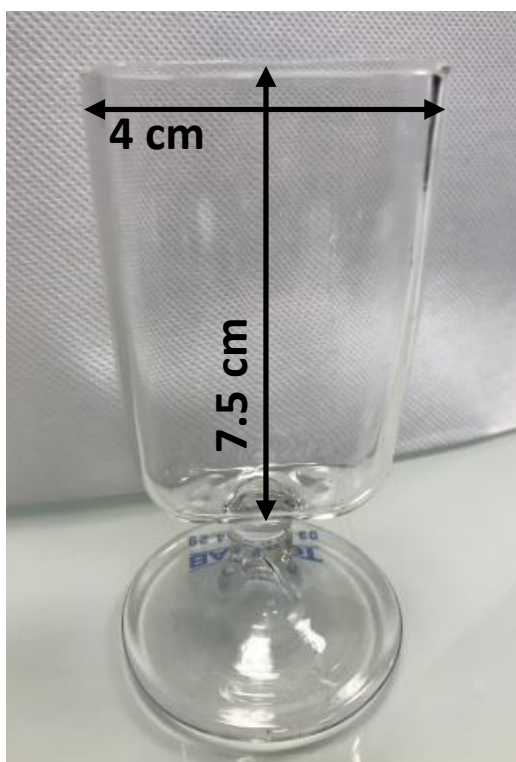


**Figure S24.** Specific piece of glass used to dip slides in the radiosensitive emulsion to perform the  $\mu$ -autoradiography experiments.

## b. $\mu$ -Autoradiography results

### *In vitro* $\mu$ -autoradiography on HeLa cells

To confirm the use of autoradiography as an efficient technique to visualise  $^{14}\text{C}$ -FLG at the cellular level, we first performed *in vitro* test by exposing HeLa cells to different amounts of  $^{14}\text{C}$ -FLG namely 0.04 kBq, 0.08 kBq, 0.16 kBq, 0.4 kBq, 0.8 kBq or 1.6 kBq, for 24 hours. To optimize resolution of the auto-radiographic images, different time of exposure to nuclear emulsion were also investigated. Interestingly,  $^{14}\text{C}$ -FLG materials were most of the time located within the cytoplasm of HeLa cells.

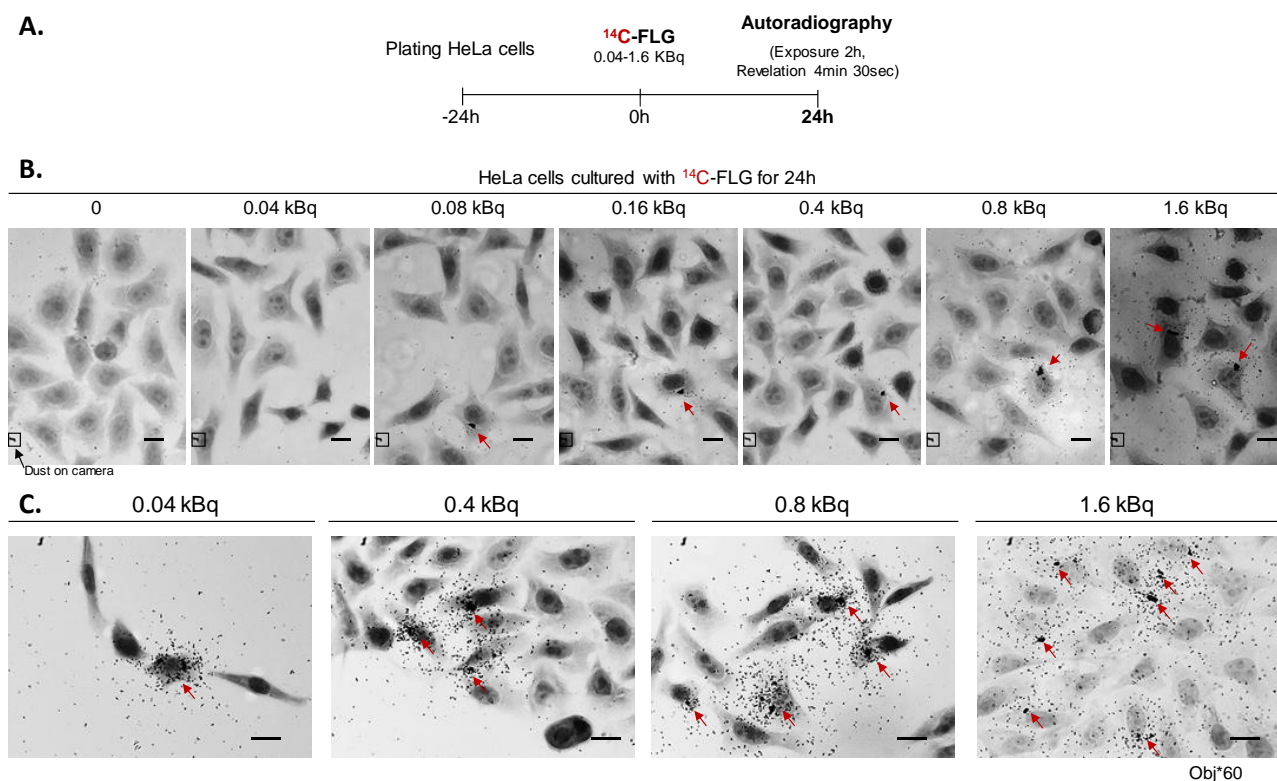
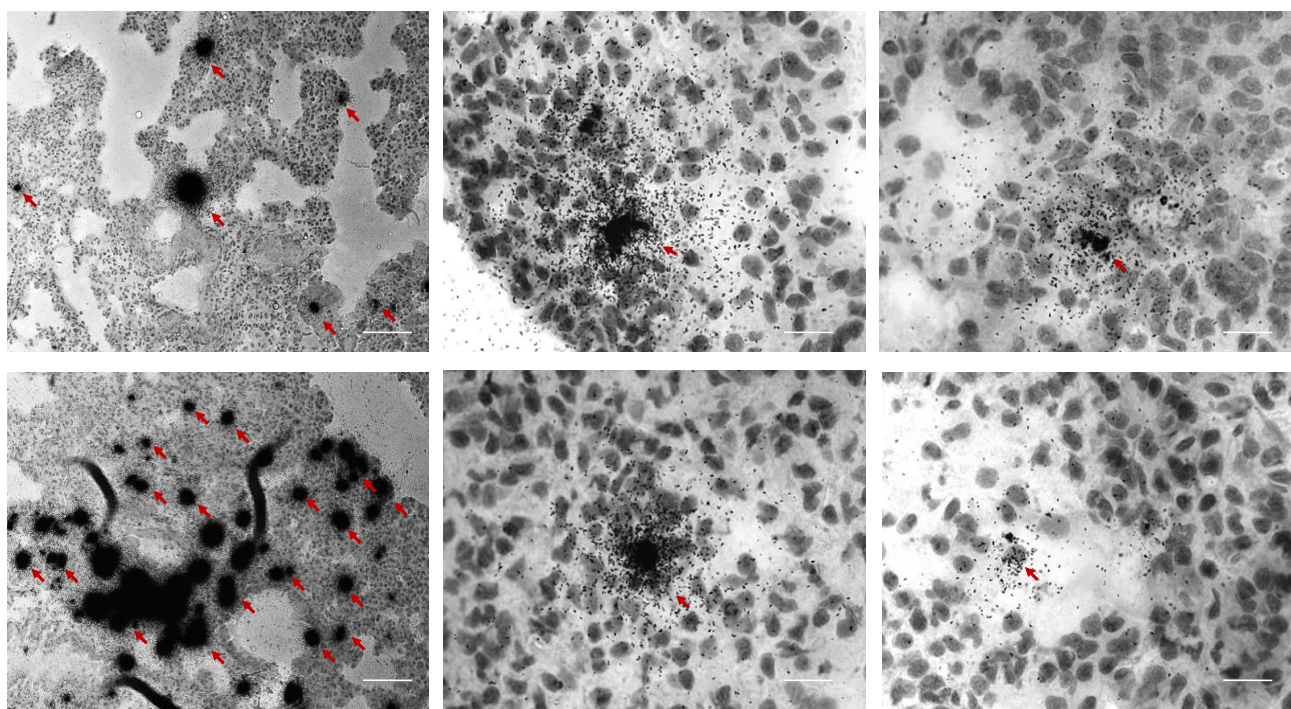


**Figure S25.** Detection of  $^{14}\text{C}$ -FLG in HeLa cells by cellular  $\mu$ -autoradiography. **A.** Experimental scheme. HeLa cells were plated and then cultured during 24h with 0 – 1.6 kBq. For this experiment, NTB emulsion was exposed only during 2h. **B.** Autoradiographs show aggregates of silver grains in some HeLa cells, indicating the presence of  $^{14}\text{C}$ -FLG. **C.** Higher magnification of autoradiographs show that aggregates of silver grains are mainly located within the cytoplasm of HeLa cells. Scale: 10  $\mu\text{m}$

## Ex vivo $\mu$ -autoradiography on tissue sections from exposed organs at 1 and 3 months

### 1. Repeated exposure

Tissue section of exposed lung (1 month)



Tissue section of exposed lung (3 months)

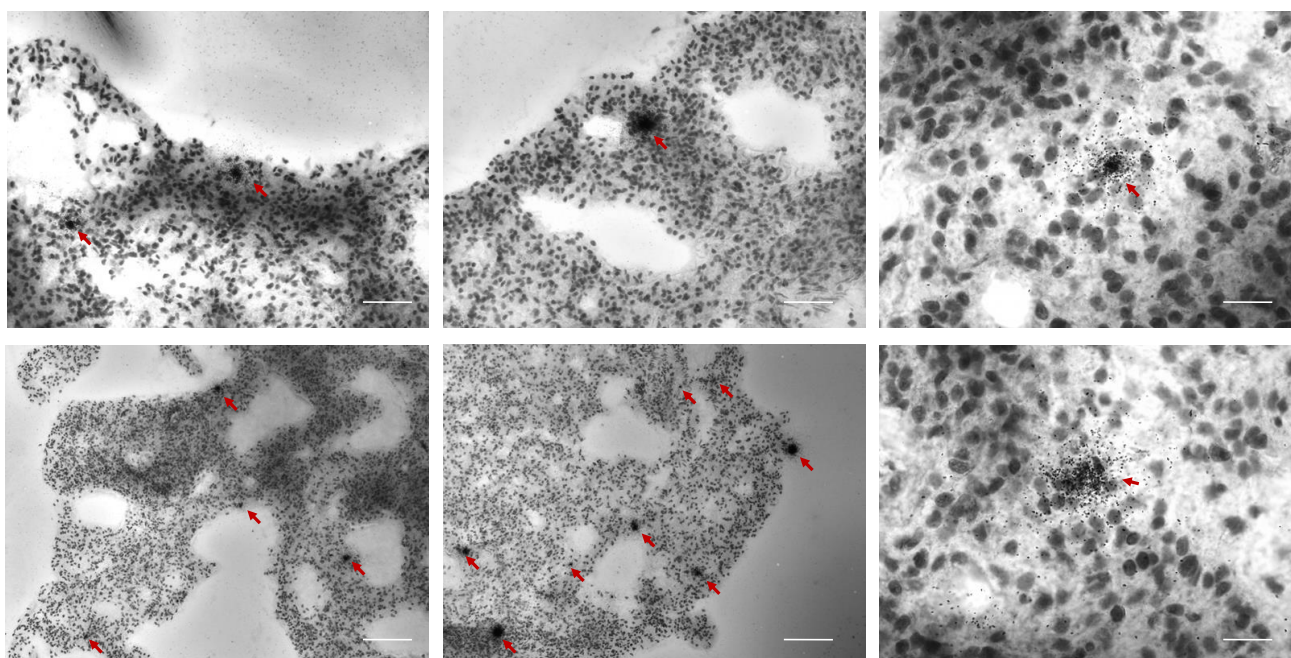
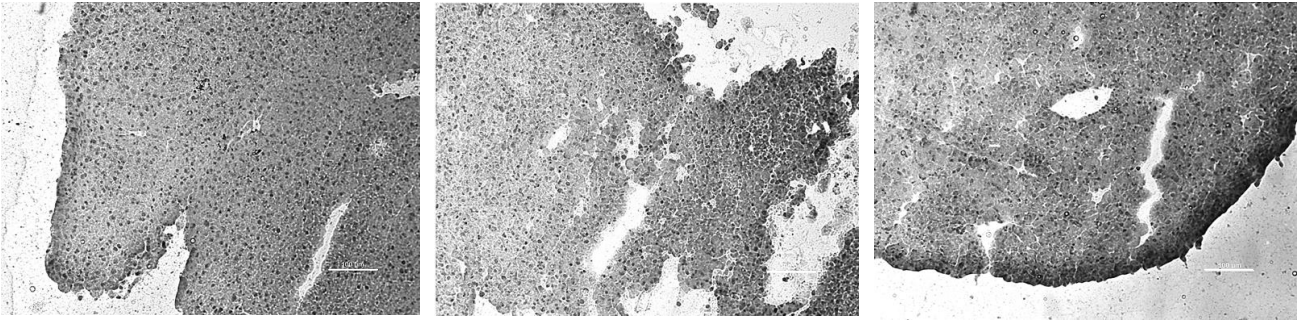


**Figure S26.** Detection of radioactivity in tissue sections of lungs after tracheal repeated exposure (at 1 and 3 months) using  $\mu$ -autoradiography. Scale: 100  $\mu$ m

Small and big black dots indicate the presence of radioactivity likely to be associated with the presence  $^{14}\text{C}$ -FLG in lungs which confirms the results provided by whole body analysis and scintillation counting.

Tissue section of exposed liver (1 month)



Tissue section of exposed liver (3 month)

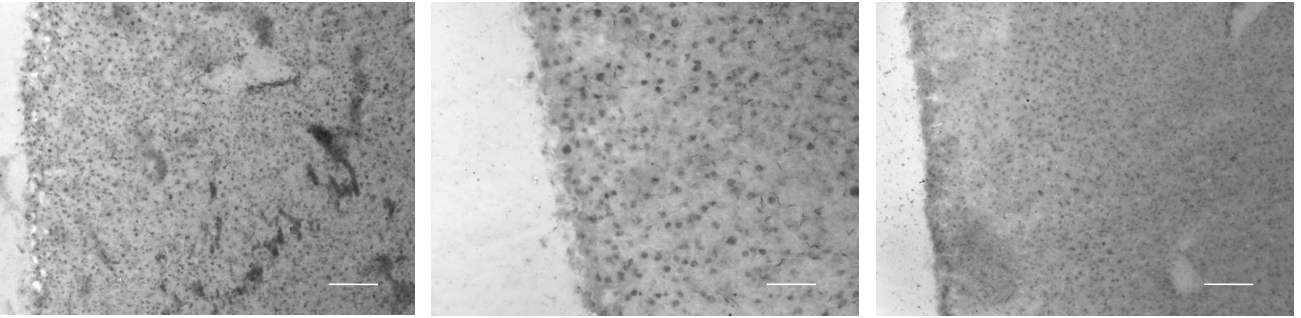


**Figure S27.** Detection of radioactivity in tissue sections of liver after tracheal repeated exposure (at 1 and 3 months) using  $\mu$ -autoradiography. Scale: 100  $\mu$ m

## 2. Single exposure

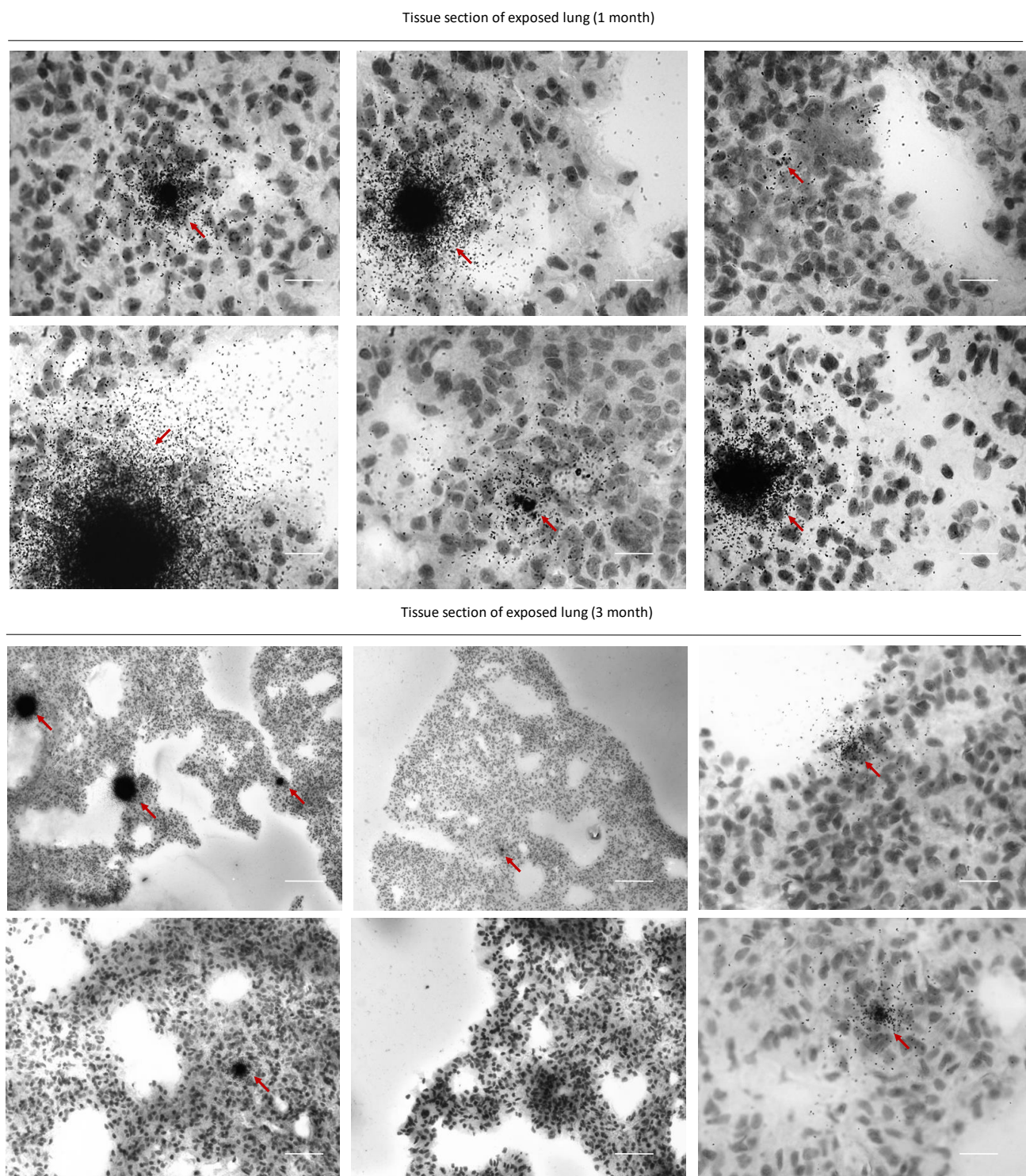
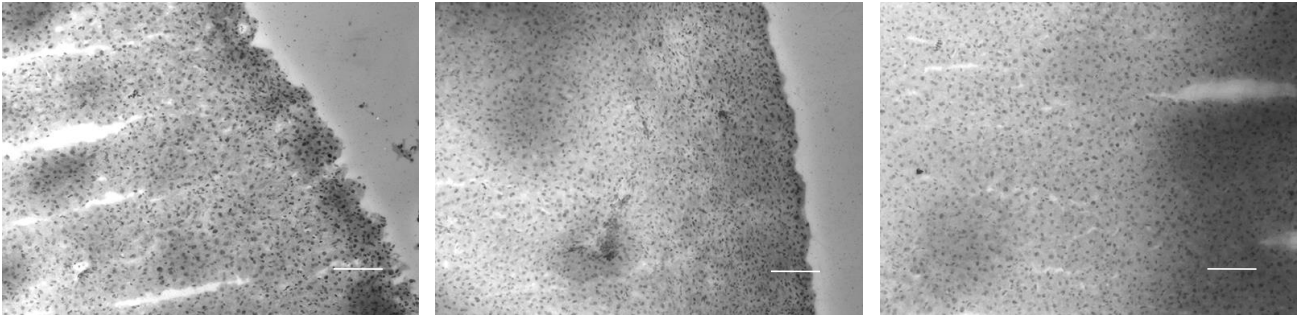


**Figure S28.** Detection of radioactivity in tissue sections of lungs after tracheal single exposure (at 1 and 3 months) using  $\mu$ -autoradiography. Scale: 100  $\mu$ m

Small and big black dots indicate the presence of radioactivity likely to be associated with the presence  $^{14}\text{C}$ -FLG in lungs which confirms the results provided by whole body analysis and scintillation counting.

Tissue section of exposed liver (1 month)



Tissue section of exposed liver (3 month)

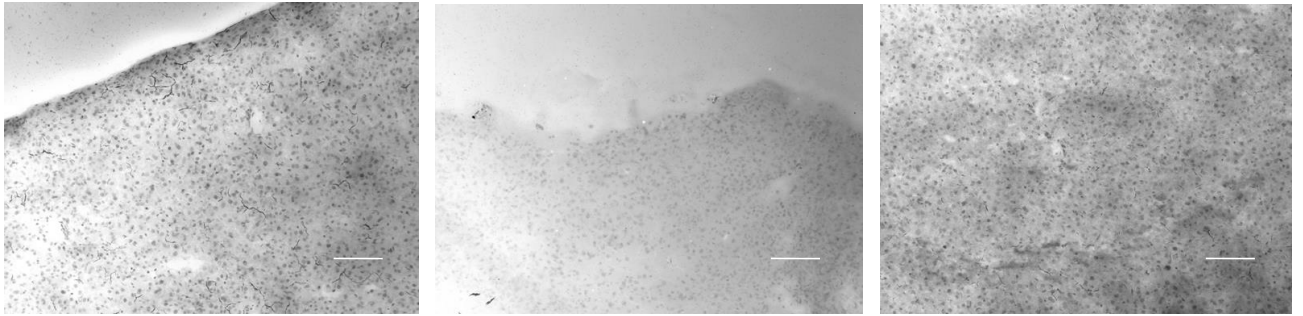


**Figure S29.** Detection of radioactivity in tissue sections of liver after tracheal single exposure (at 1 and 3 months) using  $\mu$ -autoradiography. Scale: 100  $\mu$ m

## Ex vivo $\mu$ -autoradiography on primary culture cells from exposed lungs at 1 month

### 1. Repeated exposure

Primary culture cells of lungs (1 month)

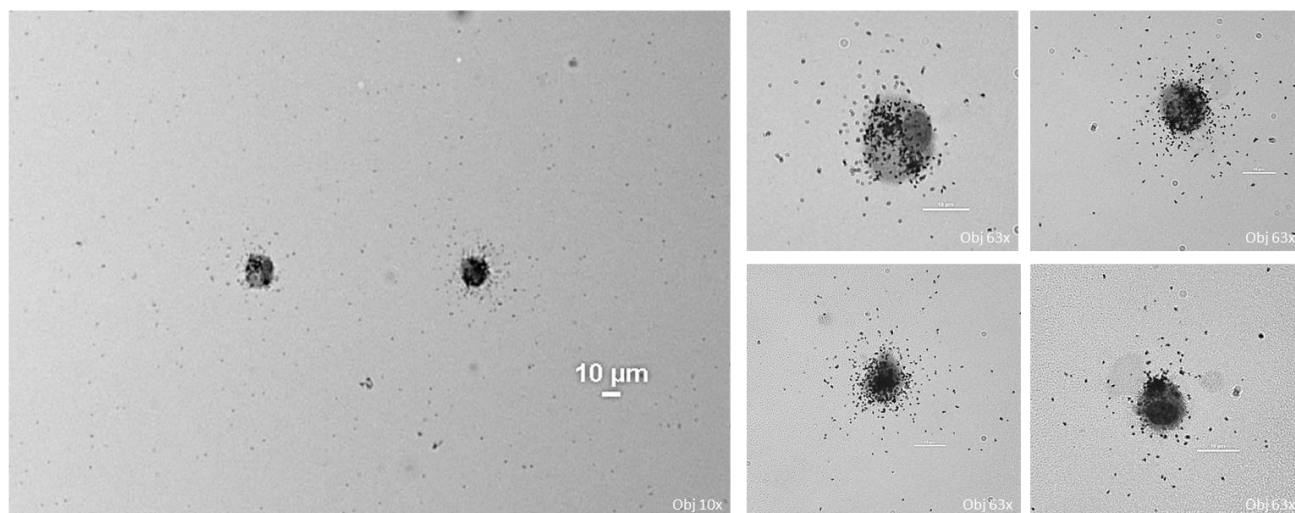


**Figure S30.** Detection of radioactivity in primary culture cells of lungs after tracheal repeated exposure (1 month) using  $\mu$ -autoradiography. Scale: 10  $\mu$ m

Small black dots indicate the presence of radioactivity likely to be associated with  $^{14}\text{C}$ -FLG which confirms the results provided by whole body analysis and scintillation counting.

### 2. Single exposure

Primary culture cells of lungs (1 month)

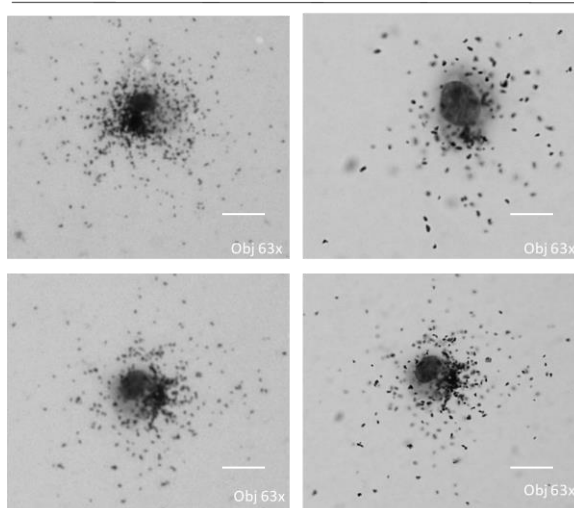
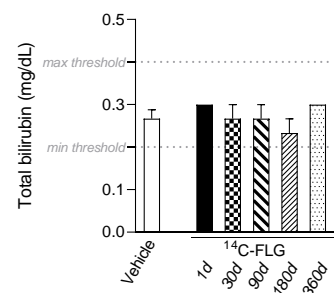
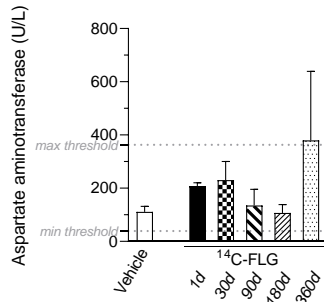
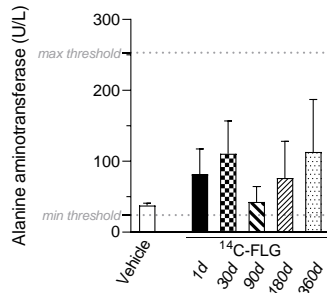


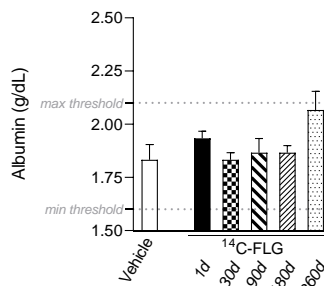
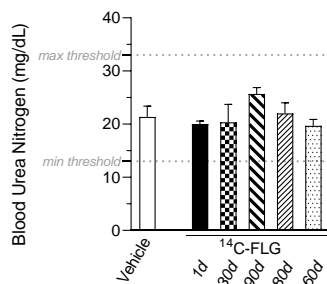
**Figure S31.** Detection of radioactivity in primary culture cells of lungs after tracheal single exposure (1 month) using  $\mu$ -autoradiography. Scale: 10  $\mu$ m

## 2.5. Toxicity

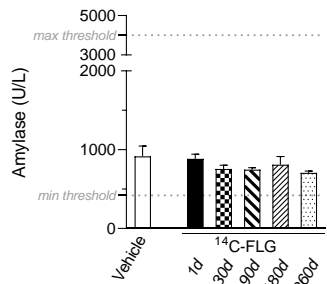
### Liver plasma parameters:



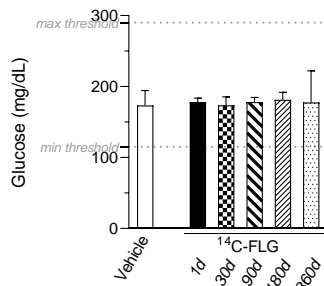
### Renal plasma parameters:



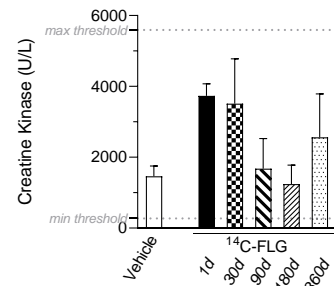
### Pancreatic plasma parameter:



### Metabolic plasma parameter:



### Muscle plasma parameter:



### Plasma electrolytes:

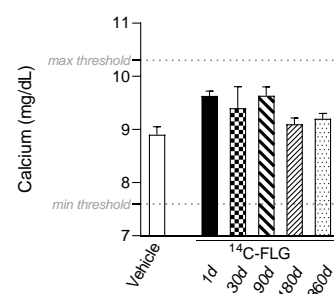
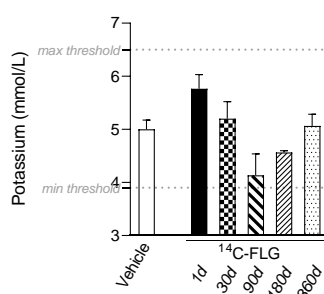
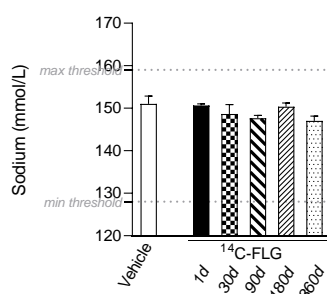
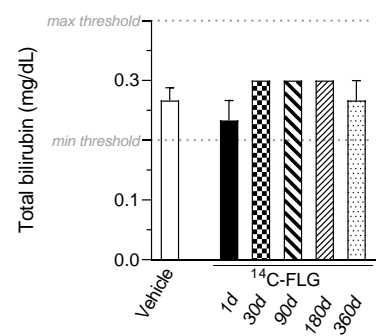
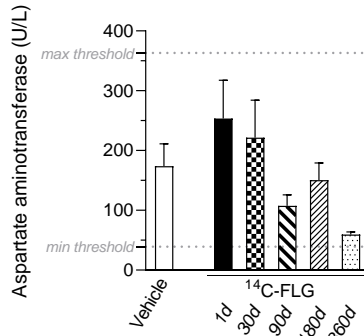
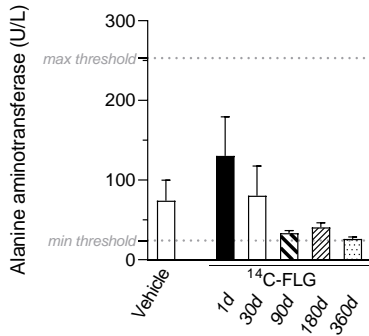
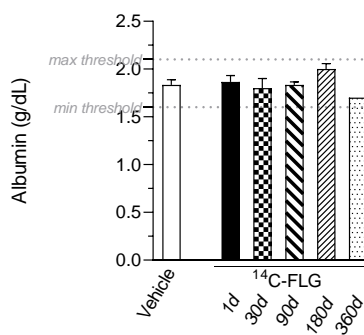
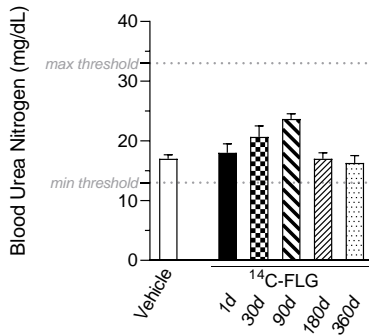


**Figure S32.** Plasmatic parameters analyzed 1d, 30d, 90d, 180d, and 360d after <sup>14</sup>C-FLG or vehicle acute administration in distinct group of mice. Thresholds (min and max) for female Balb/cJ mice are indicated in grey. Kruskal-Wallis test followed by Dunn's multiple comparisons test; ns for all parameters; *n* = 3-5 mice/group.

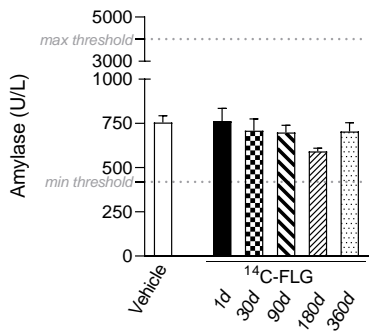
**Liver plasma parameters:**



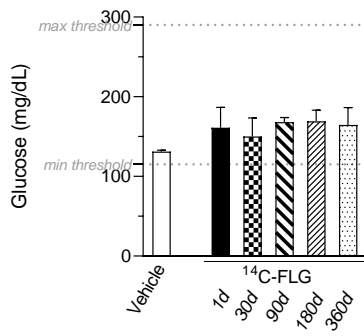
**Renal plasma parameters:**



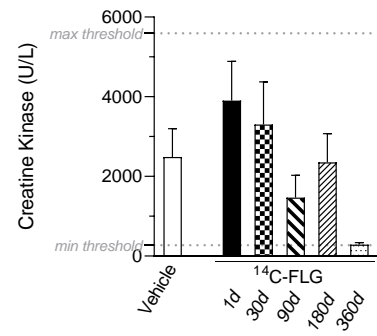
**Pancreatic plasma parameter:**



**Metabolic plasma parameter:**



**Muscle plasma parameter:**



**Plasma electrolytes:**

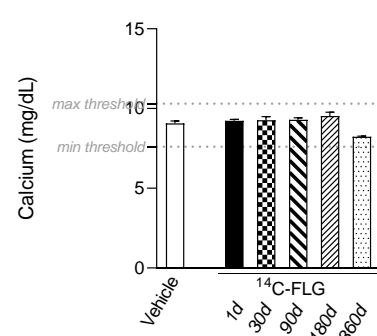
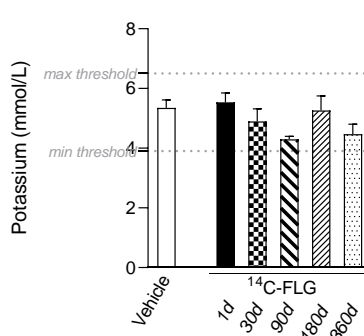
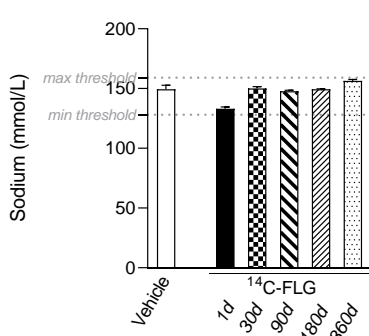


**Figure S33.** Plasmatic parameters analyzed 1d, 30d, 90d, 180d, and 360d after <sup>14</sup>C-FLG or vehicle repeated administration in distinct group of mice. Thresholds (min and max) for female Balb/cJ mice are indicated in grey. Kruskal-Wallis test followed by Dunn's multiple comparisons test; ns for all parameters; n = 3-5 mice/group.

## References

- 1 Y. Hao, Y. Wang, L. Wang, Z. Ni, Z. Wang, R. Wang, C. Keong Koo, Z. Shen, J. T. L. Thong, *Small*, 2010, **6**, 195
- 2 K. Paton, E. Varrla, C. Backes, R. J. Smith, U. Khan, A. O'Neill, C. Boland, M. Lotya, O. M. Istrate, P. King, T. Higgins, S. Barwich, P. May, P. Puczkarski, I. Ahmed, M. Moebius et al., *Nat. Mater.* 2014, **13**, 624.